

A Network Fire Model for the Simulation of Fire Growth and Smoke Spread in Multiple Compartments with Complex Ventilation

JASON E. FLOYD* AND SEAN P. HUNT

*Hughes Associates, Inc., 3610 Commerce Dr., Suite 817,
Baltimore, MD 21227-1652, USA*

FRED W. WILLIAMS

*Naval Technology Center for Safety and Survivability
Chemistry Division, Naval Research Laboratory,
Washington DC, USA*

PATRICIA A. TATEM

*ITT Industries Advanced Engineering and Sciences Division
Alexandria, Virginia, USA*

ABSTRACT: There is a need for fire modeling tools capable of rapid simulation of fire growth and smoke spread in multiple compartments with complex ventilation. Currently available tools are not capable of simulation of complex ventilation arrangements in a timely manner. To address this problem, a new fire model called Fire and Smoke SIMulator (FSSIM) has been developed. FSSIM is a network model whose core thermal hydraulic routines are based on MELCOR. FSSIM capabilities include remote ignition, multilayer heat conduction, radiation streaming, arbitrarily complex HVAC systems, detection, suppression, oxygen-limited combustion, and simple control systems.

KEY WORDS: computer model, fire, smoke, multiple compartments, HVAC.

*Author to whom correspondence should be addressed. E-mail: jfloyd@haifire.com

INTRODUCTION

A NEW FIRE model has been developed for simulating fire growth and smoke spread onboard naval vessels [1]. The core physics models are not naval specific [2]; therefore, the model is also applicable in simulating any multiple compartment enclosure. This article provides an overview of the model's core algorithms as well as shows some validation using experimental data collected from a set of single compartment fire test data and from fire testing onboard the Navy's fire test platform, the ex-*USS Shadwell* [3].

Motivation

The impetus for developing a network fire model arose from current needs of the design process for future surface combatants [4]. Fire represents a significant threat to a ship both in terms of its impact on crew health and equipment. Fire growth and spread onboard a combatant can quickly result in a loss of mission capability. Furthermore, the presence of large quantities of flammable liquids, missile propellants, and explosives onboard a typical combatant greatly increases the risk that a fire represents.

As part of the design process for future combatants, candidate designs must demonstrate that they meet specific requirements for maintaining fighting capability after a weapon hit. This is done by simulating the ship's response to a large number, hundreds to thousands, of scenarios. In addition, this simulation must account for the total ship response, which for an aircraft carrier can involve thousands of compartments. The simulation process includes accounting for direct damage from the weapon, cascading failures that result from progressive fire spread and flooding, and the damage control response of automated systems and the crew. As the designs continuously evolve, analysis needs to be rapid so that any lessons learned can be meaningfully applied to the design evolution.

Currently available computational tools do not support this process. Computational fluid dynamics (CFD), while quite capable in simulating the effects of fire, do not support rapid analysis in a cost-effective manner. Heuristic methods, rules or correlation based, while rapid, tend to be overly conservative. Existing zone models, while rapid, lack the ability to model control systems, have limitations in the complexity of ventilation systems, and were not designed for integration as a federate in a simulation environment. Thus, in order to meet the needs of the design process, the decision was made to develop a new fire model. To maximize speed, a network model approach was used.

Network Model

In the realm of computational heat and mass transfer, a network model represents the lowest level of abstraction for a multiple volume prototype. In a network model, each control volume of interest is represented as a single node. In some sense, this could be referred to as a one-zone model. For the purposes of the model in this article, a control volume is either a compartment or a heating, ventilation and air conditioning (HVAC) system component, where multiple ducts connect, for example, a tee or plenum. Heat and mass transfer occur by defining junctions between nodes. These junctions represent flow paths for the transfer of information between nodes. In the case of a flow solver, the information is mass, energy, and momentum. With one node per control volume, a network model minimizes the size of the computational space required for flow solution. This is an important consideration for a surface combatant, which has hundreds of compartments with multiple flow connections in the form of doors, hatches, and HVAC systems. A schematic diagram of the network model concept is shown in Figure 1.

A survey of existing network models for multiple compartment capabilities did not uncover an existing tool with the desired functionality. A few of these tools and their limitations are identified here. Note that none of these tools are currently designed to operate as a federate within a simulation environment.

- CFAST – CFAST is a widely used and well-validated zone model [8]. It does have many of the desired capabilities. However, CFAST's fire spread capabilities require the definition of specific objects within a space that are heated by gas phase interactions as opposed to surface contact which is a primary method of spread onboard a ship. CFAST does not allow for time-dependent flow areas for vertical flow openings. CFAST is known to have stability problems for large computations, and an entire ship simulation will have hundreds to thousands of compartments with numerous ventilation systems.
- CONTAM – CONTAM is an HVAC network model developed by the National Institute of Standards and Technology [5]. While CONTAM has numerous features supporting the computation of buoyant flows and HVAC system flows within a building, it does not contain any models for combustion-related phenomena. It also does not contain models for surface heat transfer.
- FIRAC – FIRAC was developed by Los Alamos National Laboratories, for the purpose of predicting the dispersion of radionuclides through a complex ventilation system [6]. Only a single fire can be specified in

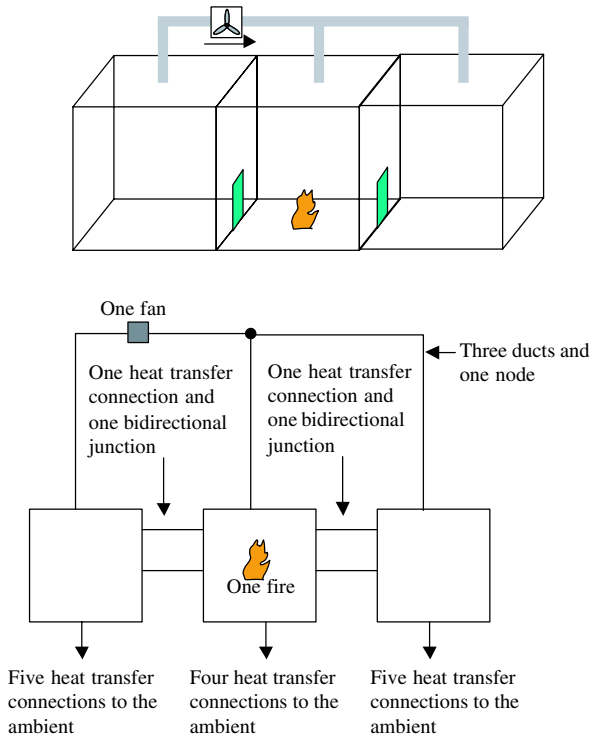


Figure 1. Network model concept. (The color version of this figure is available on-line.)

FIRAC, as its intent was to examine a single accident scenario such as a fire in a glove box. As its ultimate goal was to predict the radioactive source term, the model does not include suppression and detection, fire spread, and compartment-to-compartment heat transfer.

- **MELCOR** – MELCOR is a US Nuclear Regulatory Commission software tool for simulating the post accident response of reactor containment systems [2]. It is a network model with multiphase, multifluid capabilities as well as surface heat transfer models. MELCOR, however, does not contain any combustion, detection, or suppression models beyond a model for hydrogen deflagration.

Fire and Smoke Simulator (FSSIM)

Fire and Smoke Simulator [1] is written in standard FORTRAN 95. It runs on both Windows and Linux platforms. FSSIM uses a Fortran

namelist format for its input file, the same method of input used by Fire Dynamics Simulator (FDS) [7]. FSSIM has the following capabilities:

- 1-D flow model including friction losses and temperature-dependent specific heat.
- 1-D multiple layer, temperature-dependent heat transfer.
- N -surface, gray-gas radiation heat transfer, including radiation streaming through openings.
- Bidirectional flow through horizontal (hatches) and vertical (doors) flow connections.
- Combustion product species tracking.
- Oxygen- and fuel-limited combustion.
- Multiple user-defined fires along with fire spread via compartment-to-compartment heat transfer.
- HVAC systems including ducts, dampers, and fans with forward and reverse flow losses and multiple fan models.
- Fire detection via heat, smoke, and flame detection
- Fire spread by compartment-specific criteria.
- Fire suppression via sprinklers, water mist, gaseous agents, aerosol agents, and foam.
- Fire spread prevention via boundary cooling.
- Simple control systems to link operation of equipment to sensors or times.
- Surface leakage.
- Fast, order-real-time execution speed.

There is no practical limit other than time and available resources to the number of compartments, surfaces, vent connections, or the complexity of HVAC systems. Output from FSSIM consists of a series of comma-separated value (csv) files. The user can select groups of parameters for output, for example, compartment temperature or junction velocity, and any single parameter will be written to multiple csv files, if more than 255 columns is required, a number consistent with current csv file import limits in Microsoft Excel[®].

The overall FSSIM solver is based on the MELCOR [2] thermal hydraulic solver. MELCOR is a US Nuclear Regulatory Commission software package for performing nuclear power plant containment safety analyses. MELCOR contains a number of submodels including heat and mass transfer, spray cooling systems, deflagrations, and molten core-concrete interactions. FSSIM also includes a radiation heat transfer model based on CFAST's model [8] and a 1-D finite difference heat conduction model similar to that found in HEATING [9]. In this article, only the primary algorithms for heat and mass transfer are addressed.

Hydraulic Model

The FSSIM hydraulic solver solves the 1-D conservation equations for mass, momentum, and energy. Energy and mass are conserved explicitly; whereas, momentum is conserved implicitly. Energy conservation and mass conservation use a control volume approach, where the control volume is either a single compartment or a ventilation system node. Momentum is implicitly solved for in vent connections or in ducts.

Mass:

$$\frac{dM_i}{dt} = \sum_j \sigma_{ij} \rho_j^d v_j F_j A_j + \dot{M}_i \quad (1)$$

Energy:

$$\frac{dE_i}{dt} = \sum_j \sigma_{ij} v_j F_j A_j \rho_j^d h_j^d + \dot{E}_i \quad (2)$$

Momentum:

$$\rho_j L_j \frac{dv_j}{dt} = (P_i - P_k) + (\rho g \Delta z)_j + \Delta P_j - \frac{1}{2} K_j \rho_j |v_j| v_j \quad (3)$$

Equation of State:

$$P_i V_i = \frac{R}{mw_{\text{air}}} \frac{E_i}{c_{p_i}(T_i)} \quad (4)$$

In the above equations, i and k indicate a node (compartment or HVAC duct endpoint) and j indicates a single junction (doorway, hatch, or length of duct), note two compartments may be joined by multiple junctions. The term σ is a direction indicator, where a positive flow is defined as one exiting the compartment, d indicates a donor or upwind quantity, A represents the maximum flow of a junction, and F is the fraction of the flow area available and is utilized for time-dependent junction areas, for example, opening or closing a door. The mass and energy equations differ slightly for a duct node versus a compartment node. The FSSIM HVAC model assumes no mass or energy storage in an HVAC system. Thus, at any node in the system, mass and energy in must equal mass and energy out. Therefore, for a duct node, the time derivatives of mass and energy are zero.

The momentum equation is solved implicitly (details to be discussed later) and the mass and energy equations are solved explicitly. Hence, mass and energy will be conserved; however, momentum may not be. Since the flow fields are highly abstracted in a lumped-parameter model, many contributors to the momentum are not being captured. On the other hand, it is critical to account for toxic combustion products or the energy release from combustion.

In general, donor or upwind quantities are used in the solution. The exception is the density term in the momentum equation, where an iteration-dependent density formulation is used. If the combined pressure and buoyancy gradients are small, a change in flow direction may occur while iterating the solver. This would result in a change in the donor density, which could result in further flow oscillation. To ensure convergence in such a situation, the momentum density used is:

$$\rho_j^{n+1} = \beta \rho_j^n + (1 - \beta) \rho_j^d, \quad (5)$$

where, β is an iteration-dependent value from 0 to 1, d indicates a donor quantity, and n is the inner iteration number. For the first third of the allowed number of inner iterations, $\beta=0$, and a pure donor value is used for density. For the second third, β is varied linearly from 0 to 1. For the last third, $\beta=1$, and the density is fixed to the value at the prior iteration. Since flow oscillations can occur only if the combined pressure and buoyancy gradients across a junction are small, this typically occurs if either the densities are similar or the velocity is small. In either case, the impact of fixing the density on the solution is minimal.

The mass, energy, and momentum equations are differenced using an explicit Euler time step for mass and energy and a semiimplicit time step for momentum. The friction term in the momentum equation is approximated using a tangent/secant approach [2] to aid convergence when flow direction changes. The differenced equations as used in FSSIM are provided here.

Mass:

$$M_i^n = \left(\sum_j \sigma_{ij} \rho_j^d v_j^n F_j^n A_j + \dot{M}_i^n \right) \Delta t^n + M_i^{n-1} \quad (6)$$

Energy:

$$E_i^n = \left(\sum_j \sigma_{ij} v_j^n F_j^n A_j \rho_j^d h_j^d + \dot{E}_i^n \right) \Delta t^n + E_i^{n-1} \quad (7)$$

Momentum:

$$\begin{aligned}
 & v_j^n \left(1 + \frac{K_j \Delta t^n}{2L_j} |v_j^{n-} - v_j^{n+}| \right) - \frac{\Delta t^{n^2}}{\rho_j L_j} \frac{R}{mw_{\text{air}}} \\
 & \times \left(\frac{1}{V_i c_{p_i}^{n+}} \sum_{j1 \text{ connected to } i} \sigma_{j1} \rho_{j1}^d A_{j1} F_{j1}^n v_{j1}^n h_{j1}^d - \frac{1}{V_k c_{p_k}^{n+}} \sum_{j2 \text{ connected to } k} \sigma_{j2} \rho_{j2}^d A_{j2} F_{j2}^n v_{j2}^n h_{j2}^d \right) \\
 & = v_j^{n-1} + \frac{\Delta t^n}{\rho_j L_j} \left(P_i^{n-1} \frac{c_{p_i}^{n-}}{c_{p_i}^{n+}} + \dot{q}_i \frac{R}{mw_{\text{air}} V_i c_{p_i}^{n+}} - P_k^{n-1} \frac{c_{p_k}^{n-}}{c_{p_k}^{n+}} - \dot{q}_k \frac{R}{mw_{\text{air}} V_k c_{p_k}^{n+}} \right. \\
 & \quad \left. + \Delta P_j + (\rho g \Delta z)_j^{n-1} \right) + \frac{K_j \Delta t^n}{2L_j} (|v_j^{n+}| |v_j^{n-}|) \tag{8}
 \end{aligned}$$

The momentum equation is sufficiently complex to warrant explanation. The velocity at the next time step is determined by the average pressure difference across a junction which is computed using the compartment static pressure gradient and the junction endpoint elevations in compartments i and j . The pressure in the compartment is a function of the mass and energy flows in and out of the compartment. Thus, the velocity through a given junction is a function of the pressures in all of the compartments directly connected to the junction's endpoints through other junctions. Hence, the two summation terms in Equation (8), which account for the energy flows in the source and destination compartments. The friction term in Equation (3) was discretized as follows:

$$\frac{1}{2} K_j \rho_j |v_j| v_j \rightarrow \frac{K_j \Delta t^n}{2L_j} (|v_j^{n-} - v_j^{n+}| |v_j^n - |v_j^{n+}| |v_j^{n-}|) \tag{9}$$

where $n-$ is the prior iteration velocity, n is the next time step velocity, and $n+$ is the current guess for velocity. $n+$ will be the prior iteration value if flow direction remains constant, and it will be zero if the flow direction changes between iterations. The term $(\rho g \Delta z)$ is the buoyancy head, which is defined as:

$$(\rho g \Delta z)_j = \left((\rho_k - \rho_i) \left(z_j + \frac{1}{2} \Delta z_j \right) + \rho_i \left(z_i + \frac{1}{2} \Delta z_i \right) - \rho_k \left(z_k + \frac{1}{2} \Delta z_k \right) \right) g \tag{10}$$

Fire and Smoke SIMulator allows for bidirectional flow in both vertical (doors) and horizontal (hatches) flow connections. As mentioned earlier,

HVAC duct flows are assumed to be unidirectional. For bidirectional flow junctions, each junction is treated internally as two parallel junctions. For a doorway, the junction is partitioned according to the location of the neutral plane at the start of each time step. To avoid instabilities in the solver, the change in junction area between time steps is relaxed and no parallel junction is allowed to be <1% of the available flow area. Thus, it is possible that both portions of the junction may have the same flow direction. For a horizontal junction, the method of Cooper is used [10]. In this approach, a flooding criterion is computed for the junction. If the pressure gradient exceeds the flooding criterion, then unidirectional flow occurs. If the pressure gradient is less than the flooding criterion, bidirectional flow occurs. The momentum equation for flow in the direction indicated by the current pressure and density gradients, for example, as would occur assuming unidirectional flow, is modified to replace v_j with $v_j + v_{j,\text{ex}}$, where, $v_{j,\text{ex}}$ is an exchange flow. A correlation-based momentum equation is then used for $v_{j,\text{ex}}$:

$$v_{j,\text{ex}}^n + \frac{K_j}{2L_j} |v_{j,\text{ex}}^{n-} - v_{j,\text{ex}}^{n+}| v_{j,\text{ex}}^n = v_{j,\text{ex}}^{n-1} + \sigma_{j,\text{ex}} \frac{\Delta t^n}{L_j} \frac{1}{2} K_j \times \left(0.055 \frac{4F_j^n A_j}{\pi} \sqrt{\frac{8g\Delta\rho_j F_j^n A_j}{\pi(\rho_i + \rho_k)}} \left(1 - \frac{|\Delta P_j|}{|\Delta P_{j,\text{flood}}|} \right) \right)^2 + \frac{K_j \Delta t^n}{2L_j} |v_{j,\text{ex}}^{n+}| v_{j,\text{ex}}^{n-} \quad (11)$$

Heat Transfer

Fire and Smoke SIMulator heat transfer sub-models include correlation-based convection heat transfer; N-surface, gray gas, radiation heat transfer; and 1-D, multilayer, temperature-dependent conduction. A compartment can have as many surfaces as required to define its heat conduction paths; for example, if a compartment is adjacent to three compartments along one wall, three surfaces can be defined for that wall.

Conduction

The general equation for 1-D heat transfer in Cartesian coordinates is [11]:

$$\frac{\partial}{\partial x} \left(k \frac{\partial T}{\partial x} \right) + \dot{q}''' = \rho c \frac{\partial T}{\partial t}, \quad (12)$$

where, k , ρ , and c are all functions of temperature and position, and no heat generation. Allowing ρ to change greatly increases the computational requirements due to the impact of a varying density on noding. Thus, in FSSIM, only k and c are allowed to vary with temperature. The general equation is discretized with central differences in space and a Crank–Nicholson scheme in time [12]. The 1-D surface is divided into a series of nodes with properties defined at node centers and temperatures at node faces. Material properties are assumed constant using the prior time step temperatures, since limits on node temperature change are imposed, the impact of this is minimal. This results in the following:

$$T_i^n = T_i^{n-1} + \Delta t^n \frac{1}{(\Delta x_{i-1/2} \rho_{i-1/2} c_{i-1/2} + \Delta x_{i+1/2} \rho_{i+1/2} c_{i+1/2})} \times \frac{1}{2} \left(k_{i-1/2} \left(\frac{T_{i-1}^n - T_i^n}{\Delta x_{i-1/2}} \right) + k_{i+1/2} \left(\frac{T_{i+1}^n - T_i^n}{\Delta x_{i+1/2}} \right) + k_{i-1/2} \left(\frac{T_{i-1}^{n-1} - T_i^{n-1}}{\Delta x_{i-1/2}} \right) + k_{i+1/2} \left(\frac{T_{i+1}^{n-1} - T_i^{n-1}}{\Delta x_{i+1/2}} \right) \right) \quad (13)$$

Noding in FSSIM is determined automatically during initialization. For each material, the maximum node size to yield a Biot number of 0.1 with a heat flux of 100 kW/m² is determined. This represents the maximum node size that maintains a reasonable accuracy as a lumped parameter [7]. If the material thickness is less than this size and the surface is a single layer, then a lumped parameter heat transfer routine is used. If surface is larger than this size, the outer nodes are set to the computed value and then successively doubled going into the surface. For example, a 1-m thick surface with a Biot number thickness of 0.1 m would have node sizes of 0.1, 0.2, 0.4, 0.2, and 0.1 m. This approach is used in GOTHIC, which is another computational tool for reactor containment safety analysis [13]. This process is repeated for each layer of a surface.

At the surface boundaries, the heat transfer coefficient computed by the convection submodel and the heat flux computed by the radiation submodel are imposed. Since radiation heat transfer is highly nonlinear, the incoming radiant flux is corrected using the newly predicted surface temperatures. This is done to prevent wildly oscillating surface temperatures for insulated surfaces in flashed-over compartments. The correction is:

$$\frac{d\dot{q}_w^{\text{out}}}{dT_w} = 4\sigma\varepsilon_w (T_w^{n-1})^3 (T_w^n - T_w^{n-1}). \quad (14)$$

This results in the following discretized equation at both of the surface's boundaries:

$$\begin{aligned}
 T_1^n - \frac{\Delta t^n}{\Delta x_{3/2} \rho_{3/2} c_{3/2}} \left(\frac{k_{3/2}}{2} \frac{T_2^n - T_1^n}{\Delta x_{3/2}} \right) + \frac{\Delta t^n}{\Delta x_{3/2} \rho_{3/2} c_{3/2}} \\
 \times \left(\frac{h_1}{2} (T_1^n) + 4\varepsilon_1 (T_1^{n-1})^3 T_1^n \right) = T_1^{n-1} + \frac{\Delta t^n}{\Delta x_{3/2} \rho_{3/2} c_{3/2}} \left(\frac{h_1}{2} (2T_g^{n-1} - T_1^{n-1}) \right. \\
 \left. + q_{1,\text{rad}}^{n-1} + 4\varepsilon_1 (T_1^{n-1})^4 + \frac{k_{3/2}}{2} \frac{T_2^{n-1} - T_1^{n-1}}{\Delta x_{3/2}} \right). \quad (15)
 \end{aligned}$$

Any change in the net radiant heat transfer to the surface is accounted for in the overall compartment energy balance at the end of the time step. Thus, energy is conserved.

A tridiagonal solver is used to obtain the new temperatures. If the temperature change in any given node exceeds a user-definable tolerance, the time step is subdivided and the temperatures resolved using new thermophysical properties at the start of each sub-time step. If the flow solver undergoes an iteration, new wall temperatures are obtained using the latest radiation heat transfer solution.

Radiation Heat Transfer

Fire and Smoke SIMulator uses an N -surface, gray-gas radiation heat transfer solver similar to the solver implemented in CFAST [14]. The solver was modified to allow for streaming through large openings. The solver computes the net radiation heat transfer to the surface. This is given by:

$$\frac{\Delta \dot{q}_w''}{\varepsilon_w} - \sum_{w2} \frac{1 - \varepsilon_{w2}}{\varepsilon_{w2}} \Delta \dot{q}_{w2}'' F_{w2-w} \tau_{w2-w} = \sigma T_w^4 - \sum_{w2} \sigma T_{w2}^4 F_{w-w2} \tau_{w-w2} - \frac{c_w}{A_w}. \quad (16)$$

To prevent division by zero errors, the net radiation equation is modified as follows:

$$\begin{aligned}
 \Delta \tilde{q}_w'' - \sum_{w2} (1 - \varepsilon_{w2}) \Delta \tilde{q}_{w2}'' F_{w2-w} \tau_{w2-w} = \sigma T_w^4 - \sum_{w2} \sigma T_{w2}^4 F_{w-w2} \tau_{w-w2} - \frac{c_w}{A_w}, \\
 \times \Delta \tilde{q}_w'' = \varepsilon_w \Delta \dot{q}_w''. \quad (17)
 \end{aligned}$$

This equation results in an $N \times N$ matrix, where, N is the number of surfaces in the compartment. For most compartments, N is not very large, for example N is 0 (Equation (10)). The view factors from surface w to $w2$, F_{w-w2} , are computed assuming the compartment is a rectangular parallelepiped. Each surface defined in the input file is assigned an orientation of one of the six sides of the parallelepiped. The view factors thus take the form of two parallel rectangles or two perpendicular rectangles joined at an edge. In the event that multiple surfaces are defined along a single side, the view factor is portioned according to the area fractions of the surfaces with respect to their orientation. The source term c_w is computed by postulating a radiative fraction for the fire and transmitting it through the compartment atmosphere, accounting for absorption, using a path length that by default assumes the fire is at the center of the compartment (although the user can specify a specific location). This assumption is made, as one does not know the exact location of the fuel packages within a compartment during the design phase of a ship. Furthermore, this information, if it were available, would change in an unknown manner, following a weapon hit. Added to this is any contribution from the compartment gases. The absorption is computed using the ABSORB routine from CFAST [8].

For surfaces that are defined as being transparent to radiation, the surface emissivity is set to 1 and the surface radiation source term is set to the incoming radiation computed for the backside of the surface, for example the radiation from the other compartment. This option will result in coupling the radiation solutions of one or more compartments. To avoid construction of a single solution matrix to account for all surfaces in the joined compartments, those compartments with transparent surfaces are iterated up to five times to obtain a converged solution.

To reduce the computational burden of the radiation solver, a compartment will be bypassed if certain conditions are met. In the first velocity iteration of a new time step, the radiation solver will be bypassed for a compartment if it has no transparent surface, no pyrolysis, and its surface temperatures and gas temperatures are within 2 K of each other and <310 K. This results in a potential radiation heat transfer error of ≈ 10 W/m². In subsequent velocity iterations of a new time step, only compartments with pyrolysis or transparent surfaces are solved for. In other compartments, the potential changes in the compartment temperature during further iterations are not likely to have a significant impact on the radiation solution.

Combustion

As part of the FSSIM input, users can define one or more fires to start at explicit times. Users may also choose to allow fire to spread. Ignition of

additional fires is determined at the beginning of each time step. Each compartment can have a 'usetype' designated for it, which denotes a fuel loading and a fuel classification. Separate temperature ignition criteria can be defined for surfaces, or materials may ignite when the temperature of incoming vent flows or the compartment temperature reaches a specified value [15]. Overhead surfaces can be given a different ignition temperature from nonoverhead surfaces.

Pyrolysis is determined by one of the three methods: the fire has a constant pyrolysis rate, a t^2 pyrolysis rate, or a user-defined pyrolysis rate. The growth in pyrolysis can be limited by specifying a maximum pyrolysis rate in $\text{kg}/\text{m}^2\text{s}$. All fires can be given an end time in either absolute time or fuel loading. The calculated pyrolysis rate can be reduced by various mechanisms including suppression and oxygen availability.

Combustion of pyrolyzed fuel is calculated on the basis of the available oxygen, defined by a user-defined, constant, LOI, in the compartment where the pyrolysis is occurring. Currently, there is no burning of unburnt fuel exiting one oxygen-depleted compartment into a second oxygen-rich compartment, though the unburnt fuel is tracked. If there is sufficient oxygen in the compartment above a user-specified lower limit, all the pyrolyzed fuel will combust. If there is insufficient oxygen in the compartment, a more detailed estimate of the available oxygen is made which includes a prediction of the net inflow of oxygen based on prior time step velocities. The actual heat release rate is adjusted to use the calculated amount of available oxygen. Note that a fire in an oxygen-depleted compartment can burn at a rate equal to the pyrolysis rate if there is a sufficient flow rate of oxygen into the compartment.

Species are generated based on user-provided yields for each fuel being burned. These yields represent the mass of combustion products formed for a unit mass of fuel burned. Note that the consumption of oxygen can be expressed as a negative yield. Currently, unburned fuel is tracked as a species, but no separate model is present to burn it in downwind compartments.

Solution Algorithm

The FSSIM solver consists of a time step initialization, an outer loop, and an inner loop. The overall program flow is shown in Figure 2. The outer loop monitors the overall convergence of the time step and limits the maximum relative change in thermophysical conditions over a time step. The inner loop handles the solution of the velocity and those parameters required for the velocity computations.

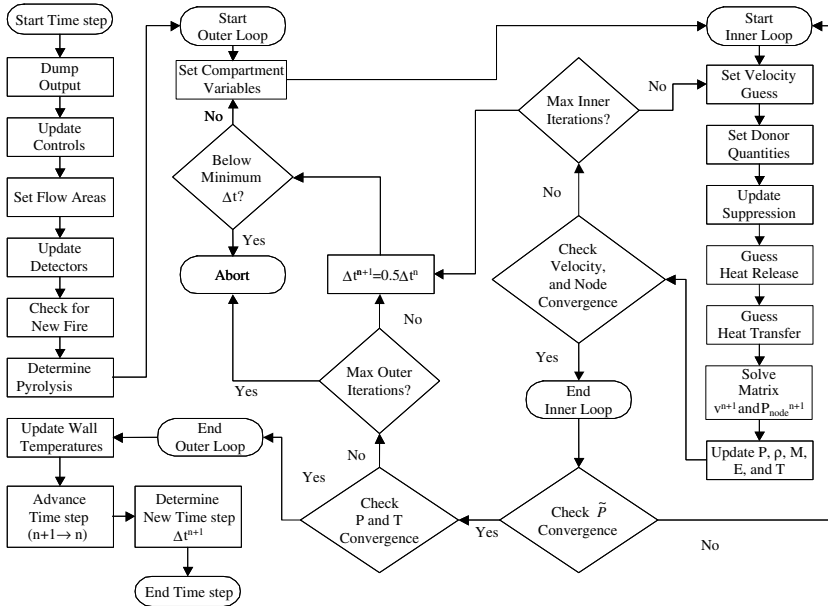


Figure 2. FSSIM flowchart.

Time Step Initialization

The time step initialization computes those parameters that do not change during either outer loop or inner loop iterations. This is followed by recursively updating control functions, which allows for functions of control functions to be specified. Junction flow areas, the status of detection systems, the ignition of new fires, and the computation of pyrolysis rates are performed during the time step initialization. The outer loop is then entered, and upon return, the time step is advanced.

Outer (Pressure) Loop

The outer loop monitors the overall convergence of the time step solution and computes the final predicted values of updated quantities. It begins by estimating the compartment specific heats for the end of the current time step using the current heat and mass transfer solution. The inner loop is then executed. Upon return from the inner loop, the end of time step pressure is compared to a predicted end of time step pressure that is computed using the prior iteration heat and mass transfer solution. A large discrepancy between

the two indicates that thermophysical conditions are changing rapidly in some portion of the domain and the outer loop is repeated to ensure that the solution has converged. Next, the relative change in temperature and pressure for each node as well as the fraction of mass exchanged for each compartment are determined. If any of these exceed user-definable stability limits, the outer loop is repeated with a smaller time step. If the solution is successful, a new time step size is determined using the quantity and parameter closest to its stability limit as a guide. The maximum allowable increase in step size is a factor of two. If the maximum number of outer iterations is exceeded, the code will abort.

Inner (Velocity) Loop

The inner loop contains the bulk of the computations for FSSIM. It begins by determining the velocity solution guess (see the text for Equation (9)) followed by setting donor quantities. Suppression systems are updated and guesses are made for heat transfer and combustion. If a compartment is underventilated, combustion will be limited to the incoming oxygen with a relaxation on the maximum changes in heat release rate between iterations. Since pressure and velocity are tightly coupled, and since the heat release as a momentum source is strongly dependent on inflowing air, the relaxation reduces oscillations in heat release rate. With all momentum source terms updated, the momentum solution matrix is constructed and solved. This is followed by updating the end of time step quantities. If any junction velocity changes sign or magnitude by a user-definable criterion, the inner loop is repeated. Heat release rates are recomputed only in underventilated compartments. If the maximum number of inner iterations is exceeded, the time step is reduced by 50% and the outer loop is cycled.

There are three submodels that require solving a system of linear equations in the inner loop. They are the surface heat conduction solver, the radiation heat transfer solver, and the velocity solver. While each surface could have many nodes, the matrix is tridiagonal and the solution is rapid. The radiation solver involves a dense matrix, so sparse solution techniques cannot be used. Therefore, LU decomposition is used. Fortunately, a typical shipboard compartment has less than a dozen surfaces. For a large geometry with many junctions, the flow matrix could become quite large and computationally expensive to solve. To reduce computational time, two optimizations are made. The first optimization determines if any hydraulically separate regions exist. For example, if the geometry consisted of a single row of ten compartments with connecting doors with all doors open except for the one between compartment 5 and 6, there would be two

hydraulic regions. The flow solver will loop over each hydraulic region, including in the matrix only those junctions present in the region. Regions are redetermined if any door or duct has its area changed to or from zero due to a control function operation. The second optimization removes any zero value rows or columns from the flow matrix. This can occur if the user specifies a fixed flow for an HVAC system as opposed to a set of ducts and fans with fan curves and duct losses. Last, since any compartment is typically connected directly only to a small number of compartments, the matrix tends to be sparse. A sparse solver is used for the velocity solution when $N > 25$. As an example of FSSIM's speed, recent use of FSSIM for an input geometry with 2000+ compartments, 3000+ flow connections, and 12000+ heat transfer surfaces had a simulation time to run time ratio of 1:8. For the more modest simulation presented later in this paper with 20+ compartments, 250+ flow connections, and 150+ heat transfer surfaces had a ratio of 3:1.

Assumptions and Limitations

The major assumptions made in FSSIM with a discussion of the potential limitation for each assumption are presented here. It is noteworthy that there are no realistic limitations, other than those imposed by CPU, memory, and time limitations, on the number of compartments, surfaces, etc. that can be specified in the input:

- Compartments are represented by a single set of quantities (temperature, species, etc.).

For a compartment where the fire size is small compared to the compartment volume and where good ventilation is present, stratification will occur in the space (e.g., two layers). In this case, heat transfer to the overhead will be underpredicted and that to the deck overpredicted. However, fires of this sort are not likely to pose a significant thermal threat to the remainder of a structure. Also, as mentioned later in this article, FSSIM can predict correct vent flow conditions for this case ensuring that any tenability effects are reasonably captured. Beyond the burning compartment, vent flows act to mix the gas volume of a compartment and stratification is less pronounced.

- HVAC ducts have unidirectional flow with no mass or energy storage.

When a ventilation system is running, the unidirectional flow assumption is valid. When a system is off, bidirectional flow within ducts is possible; however, the flow losses in a typical HVAC system work against any significant flow due to buoyancy effects. The mass and energy storage assumption results in faster transfer of mass and energy to

remote compartments. Since increase in temperature and smoke density is a negative outcome, this assumption is conservative.

- Convection heat transfer is a function of the bulk temperature and surface orientation.

This is the same assumption used in CFAST. Enhanced convection from fires against walls or in corners is not accounted for. Thus, potential hot spots on surfaces are not being resolved. Therefore, fire spread predictions may not be correct for specific fuel configurations, where a fire exists on one side of a surface directly opposite a fuel source on the other side of the surface. However, the specific location of fuel within a compartment is typically not known during the phases of design in which simulation tools are applied.

- Combustion product yields are constant regardless of stoichiometry.

Results of compartment fire research have indicated that the combustion product yields within a compartment are not a trivial function of the equivalence ratio, but rather are also dependent on geometric effects [16]. Thus, for a lumped parameter model, there is no guarantee that a specific functional relationship will be accurate for all fuels and equivalence ratios. However, the user is free to specify yields with any desired degree of conservatism.

- The vector for gravitational acceleration is fixed in the $-z$ -direction.

For a building, this will be a correct assumption. However, a ship has list and trim, which is a function of the sea state, the ship's speed and course, and the current ballasting of the ship. Thus, the vector for the ship's vertical axis and gravity will not always coincide. Impacts from wave actions are quasi-periodic with a minimal average effect. Effects resulting from ballasting or progressive flooding, however, are persistent with time. The goal is to keep these effects to a minimum as a severe list can cause stability problems that capsize a ship. For cases where stability is not the overriding concern, list or trim will be a small deviation from the vertical axis and not have a significant impact on buoyancy computations.

VALIDATION

Data Reduction

Temperature in FSSIM is an expression of the energy content of the volume of gas in a compartment including the hot gas layer, the fire plume, the flaming region, and any unentrained cold gas layer that might be present. A real compartment exposed to heat from a combustion process will not have the same temperature everywhere throughout the compartment.

Instead, temperature will vary throughout the compartment. To compare FSSIM to experimental data on an equal footing requires determining the energy content of the compartment and the mass of gas in the compartment. Combining these parameters can yield an effective temperature. In a given set of experimental measurements of compartment temperature, it is assumed that each measurement represents the energy content of a volume of gas surrounding that location. It is also assumed that the gas in the compartment follows the ideal gas law and has a molecular weight of air. The total energy content of the compartment can be expressed as:

$$E = \sum_n V_n \rho_n c_{p,n}(T_n) T_n = c_p(\bar{T}) \bar{T} \sum_n V_n \rho_n, \quad (18)$$

where n represents a temperature measurement location, V is the volume, ρ is the density, c_p is the specific heat, and T is the temperature. Applying the ideal gas law and assuming a constant specific heat and isobaric conditions inside the compartment yields:

$$E = \sum_n V_n \frac{mw_{\text{air}} P}{RT_n} c_p T_n = c_p \bar{T} \sum_n V_n \frac{mw_{\text{air}} P}{RT_n} \Rightarrow c_p \sum_n V_n = c_p \bar{T} \sum_n \frac{V_n}{T_n} \quad (19)$$

$$\bar{T} = \frac{\sum_n V_n}{\sum_n V_n / T_n} \quad (20)$$

Single Compartment with a Vent

This test series consisted of 55 methane fires in a single compartment with one opening performed at the National Bureau of Standards' Center for Fire Research, now the National Institute of Standards and Technology's Building and Fire Research Laboratory [17,18]. Fire size, fire location, and opening size were varied. The compartment was $2.8 \times 2.8 \times 2.13 \text{ m}^3$ and was lined with ceramic fiberboard. The compartment was instrumented with a fixed, internal rake of 19 aspirated thermocouples and a movable rake of 17 bare thermocouples, and 18 bidirectional probes. The movable rake was positioned in the doorway. From this instrumentation, one can determine the average compartment temperature, the mass flow rate exiting the compartment, and the location of the opening's neutral plane. Fire heat release rates (HRR) in the test series ranged from 31.6 to 158 kW. Opening width and sill height were varied with the soffit height fixed at 1.83 m. FSSIM, CFAST, and FDS were used to model a subset of these tests. The subset modeled is described in Table 1.

Table 1. Summary of NBS compartment fire tests modeled.

Test ID*	Ambient (K)	HRR (kW)	Sill (m)	Width (m)	Test ID	Ambient (K)	HRR (kW)	Sill (m)	Width (m)
10	296.05	62.9	0.00	0.24	20	302.85	105.3	0.00	0.74
11	298.35	62.9	0.00	0.36	21	301.90	158.0	0.00	0.74
12	292.50	62.9	0.00	0.49	22	299.75	62.9	0.45	0.74
13	293.10	62.9	0.00	0.62	23	296.15	62.9	0.91	0.74
14	301.55	62.9	0.00	0.74	30	296.15	62.9	0.91	0.74
16	296.70	62.9	0.00	0.86	41	287.15	62.9	0.00	1.37
17	291.90	62.9	0.00	0.99	612	296.15	62.9	0.00	0.49
18	302.30	62.9	0.00	0.74	710	288.15	62.9	0.00	0.74
19	302.15	31.6	0.00	0.74	810	286.15	62.9	0.00	0.74

*Italic test ID indicates test simulated with FDS.

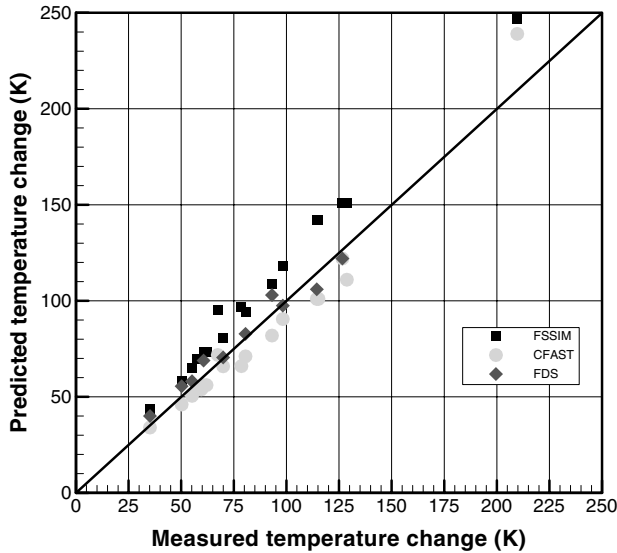


Figure 3. Predicted vs measured average compartment temperature for NBS compartment.

Figures 3–5 show the results of the FSSIM computations versus the test data along with results from CFAST and FDS computations. Figure 3 shows the net temperature change inside the compartment; note that the measured data, CFAST predictions, and FDS predictions were reduced using Equation (20). Figure 4 shows the mass flow rate out of the compartment. Figure 5 shows two related comparisons. For FSSIM and FDS, Figure 5 shows the calculated versus measured neutral plane

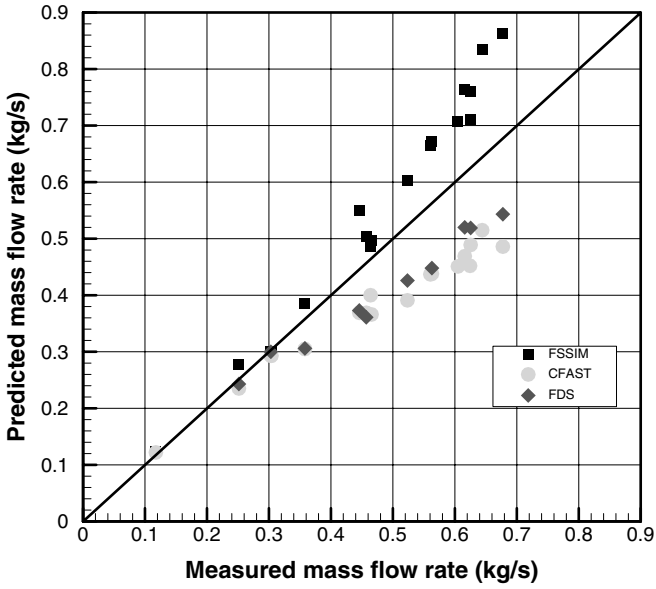


Figure 4. Predicted vs measured vent mass flow rate for NBS compartment.

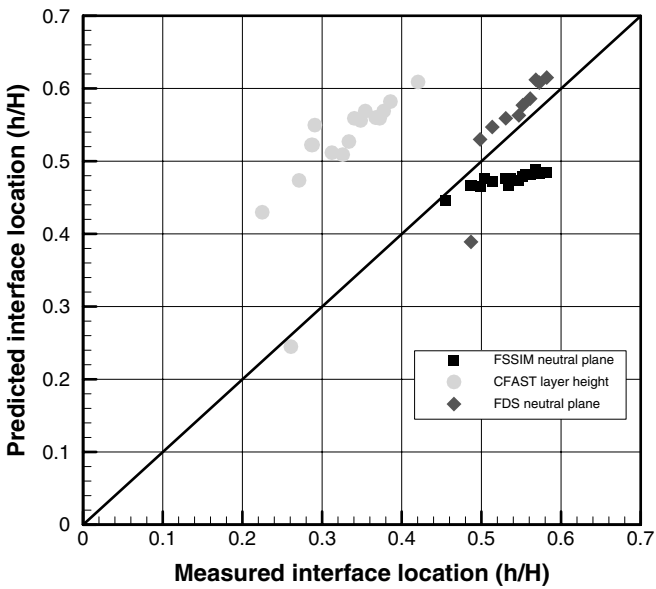


Figure 5. Predicted vs measured normalized interface height for NBS compartment.

Table 2. Summary of prediction errors for NBS compartment fire tests.

Quantity	FSSIM	CFAST	FDS
Temperature			
Min error (%)	15	3	1
Max error (%)	41	16	14
Avg error (%)	21	9	7
Massflow			
Min error (%)	1	3	1
Max error (%)	29	28	21
Avg error (%)	14	18	15
Interface			
Min error (%)	2	6	3
Max error (%)	17	91	20
Avg error (%)	11	60	7

normalized by the vent opening height. Since CFAST outputs only the layer height, Figure 5 shows the CFAST calculated versus measured layer height normalized by the compartment height.

In Figures 3–5, FSSIM accurately predicts the overall trends in the data for each of the three quantities. FSSIM also accurately predicts the magnitude of the data. It also predicts the quantities with similar or less error magnitude than CFAST, though it does not predict as well as FDS. Table 2 shows the prediction errors of the three programs relative to the measured data. The average errors for all the FSSIM-predicted quantities are <20%.

Ex-USS *Shadwell* 688 Sub Test Series

During 1995 and 1996, a series of tests were conducted in a modified portion of the port wing wall of the ex-USS *Shadwell* (LSD-15) [3]. The port wing wall was modified to represent the forward section of a Los Angeles (SSN 688) class attack submarine. In total, 108 tests were performed within the test area to evaluate the existing doctrine and tactics under prototypical fire conditions and to evaluate alternative approaches to maintaining tenability of key spaces [19]. The submarine test area is shown in Figure 6.

The submarine test area contained twenty-three compartments, four of which were dead air volumes, encompassing over 1000 m³ of free air volume [20]. The active compartments were connected by fourteen hatches and scuttles, eleven doorways, three ventilation systems, and eight frame bay openings (vertical ducts connecting the laundry room and torpedo room to the control room and combat systems space). The ventilation systems were a supply system, an exhaust system, and a smoke control system with

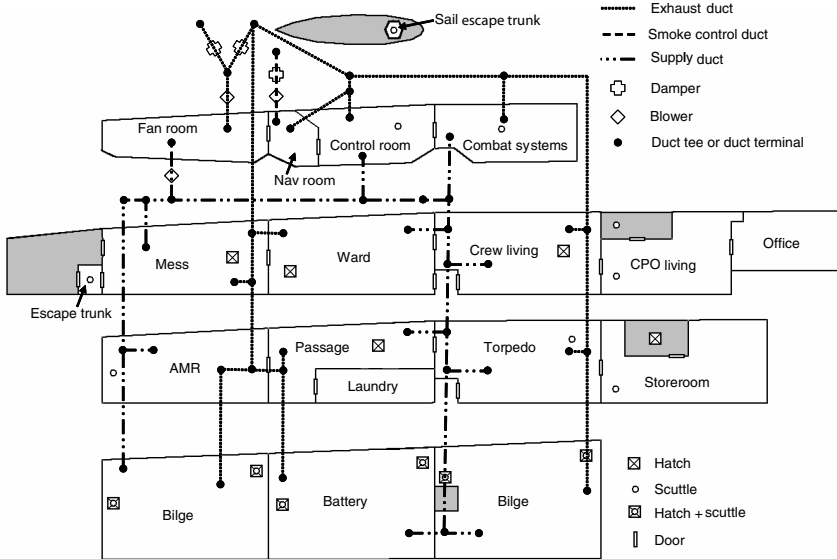


Figure 6. Diagram of the Ex-USS Shadwell 688 submarine test area depicting flow connections and HVAC system connectivity (shaded regions are dead air volumes).

a combined total of three fans, three dampers, and 48 distinct segments of ducting. There were three modes of operation for the ventilation system. The first mode is recirculation with the supply system taking suction from the fan room and discharging to the test area, and the exhaust system taking suction from the test area and discharging to the fan room. The second mode is a surface ventilation mode. In this mode, the supply fan operates as before taking air from the fan room and distributing it through the compartments. The exhaust fan is aligned to take suction from above the sail (weather). Note that this mode also requires that one or more of the topside hatches be open to serve as an exhaust location. The final mode is an emergency ventilation mode where the supply and exhaust systems are secured, and a smoke control system activates that takes suction from the Navigation Equipment Room and discharges above the sail (weather). The last two modes require opening an external hatch to serve as discharge in the surface ventilation mode and an intake in the emergency ventilation mode.

A handful of the 108 tests used wood cribs for the fire source; the remainder had diesel pool fires. Fires were placed in a variety of locations in the test area with a majority of the tests having fires in the laundry room. Fire size, location, ventilation conditions, and, for some tests, manned

response were varied. Approximately 360 channels of data were collected for each test, including selected hatch, duct, and doorway velocities; gas and surface temperatures; species concentrations; and visibility.

Fire and Smoke SIMulator was used to model the first 20 min of test 5-14, which was a 250 kW diesel fire in the laundry room with the frame bays open, the escape trunk hatch to the ambient open, and the ventilation system switching from normal recirculation to emergency ventilation at 1 min after ignition. Volumes, wall surface areas, wall thicknesses, flow connections, and HVAC properties (duct sizes, flow losses, and fan curves) were provided in the form of a digital database representation of the submarine test area. In total, the FSSIM input file included 23 compartments, 20 open doors and hatches, 56 ducts, 67 HVAC nodes, 3 fans, and 171 heat transfer surfaces with seven steel thicknesses. Surface leakage was enabled on all the interior surfaces resulting in an additional 65 flow connections. The simulation was performed on a 2 GHz PC running Windows® 2000, and 20 min of simulation took 7 min of CPU time.

Modeling was not performed using either CFAST or FDS. With FDS, the complexity of the ventilation systems and the resolution needed for the number of compartments would have made a model very costly in terms of computational resources and time. A CFAST model was attempted; however, the complexity of the ventilation system and size of the overall geometry resulted in stability problems. Since the compartments in the sub test area are coupled through the many vent openings and ducts, a simpler CFAST model would not have made for a meaningful comparison with FSSIM and the measured data.

Figure 7 shows the predicted and measured temperature changes for the control room. Both individual experimental thermocouple measurements are shown along with the average temperature. The control room was connected directly to the laundry room by two frame bay ducts. Two additional ducts connected the control room to the laundry room passageway. Therefore, even though this space is two levels above the laundry room, it saw a relatively rapid increase in temperature. The FSSIM predictions for the control room are slightly lower than measured in the data, 7 K (10%) lower temperature change. The predictions match the overall temperature-rise trend well.

Figure 8 shows the average measured temperature and the predicted temperature change for a number of compartments in the sub test area. In general, FSSIM is matching both the magnitude and the time-dependent rate of rise for all the spaces shown. As can be seen from Figure 6, these spaces span the sub test area. The storeroom, navigation room, and laundry passage each had one rake of five thermocouples. The remaining compartments each had two rakes of five thermocouples.

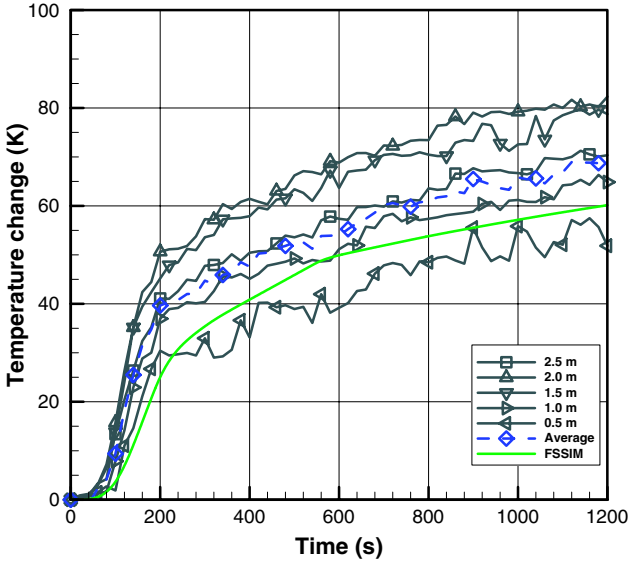


Figure 7. Predicted vs measured control room temperature changes for Shadwell/688 test 5-14. (The color version of this figure is available on-line.)

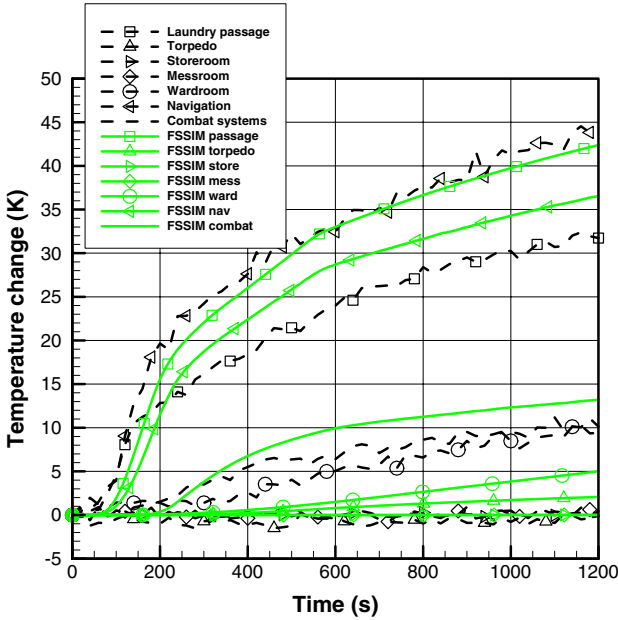


Figure 8. Predicted vs measured temperature changes for Shadwell/688 test 5-14. (The color version of this figure is available on-line.)

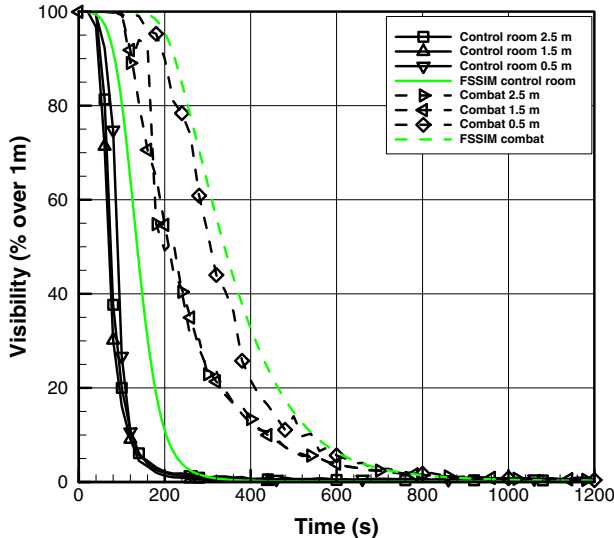


Figure 9. Predicted vs measured control room and combat systems visibility for Shadwell/688 test 5-14. (The color version of this figure is available on-line.)

Figures 9 and 10 show visibility and oxygen concentrations, respectively. Visibility, in terms of percent transmittance over 1 m, is shown for the control room and combat systems space, where each compartment had three visibility measurements made using laser over a distance of 1 m at heights of 2.5, 1.5, and 0.5 m above the floor. FSSIM predicts a similar time dependent rate of change of visibility and correctly predicts that the control room visibility decreases approximately twice as fast as the combat systems space. The time delay before an observable decrease begins is also correctly predicted. The oxygen concentration measurements were made at two locations in both the control room and the laundry room. The periodic spikes in the measured data result from using compressed air to periodically purge the gas sampling lines during the test. It was anticipated that FSSIM would predict a slightly lower oxygen concentration in the laundry room than measured, because even if all other quantities (total energy and mass flow) were correctly predicted, the measured data would not capture the highly oxygen-depleted region within the plume. FSSIM predicts a lower concentration than measured. However, FSSIM predicts a higher concentration in the control room than measured. The measured data, regarding both oxygen and visibility, indicate that the space is well-mixed. The combination of these two factors indicates that FSSIM is not transporting enough mass from the laundry room to higher levels in the sub test area.

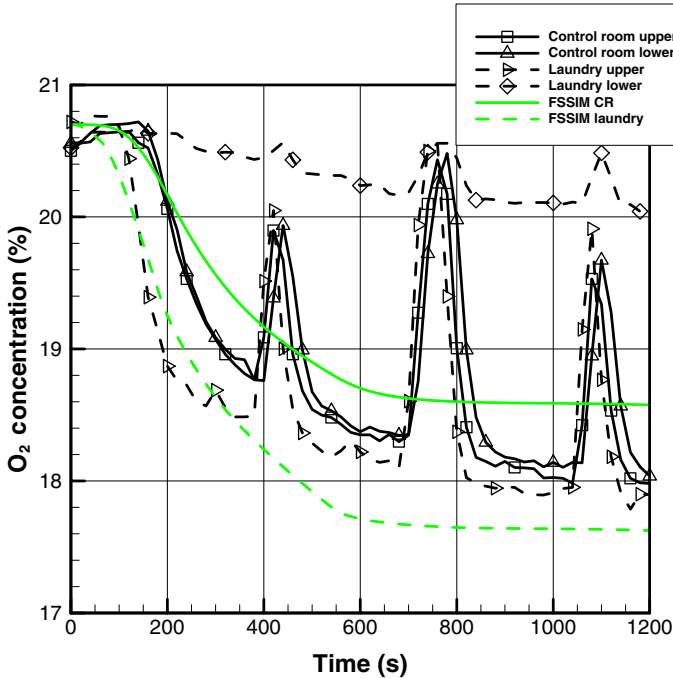


Figure 10. Predicted vs measured control room and laundry room oxygen concentrations for Shadwell/688 test 5-14. (The color version of this figure is available on-line.)

Figures 11 and 12, respectively, show predicted and measured velocities in the frame bays and in the primary ducts of the HVAC system. In Figure 11, velocities are shown for four of the eight frame bays; there were two side-by-side in each of the four locations. FSSIM correctly predicts both the magnitude and the direction of the flow in the frame bays. In Figure 12, velocities are presented for four locations in the HVAC system. These locations are: in the duct connected to the supply blower used during normal recirculation mode, in the duct connected to the exhaust blower used during normal recirculation mode, in the duct connected to the low pressure blower used during the emergency ventilation mode, and in the bypass duct used as an external fresh air supply (induction) during the emergency ventilation mode. The FSSIM predicted velocities in these ducts are being computed from first principles using manufacturer-supplied fan curves and the flow losses and lengths associated with all the individual components in the HVAC system. Considering this, the FSSIM predictions are excellent.

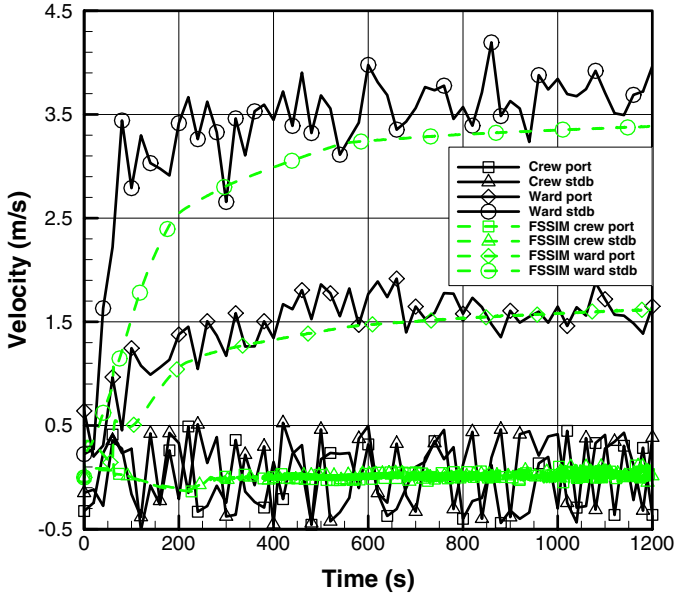


Figure 11. Predicted vs measured frame bay velocities for Shadwell/688 test 5-14. (The color version of this figure is available on-line.)

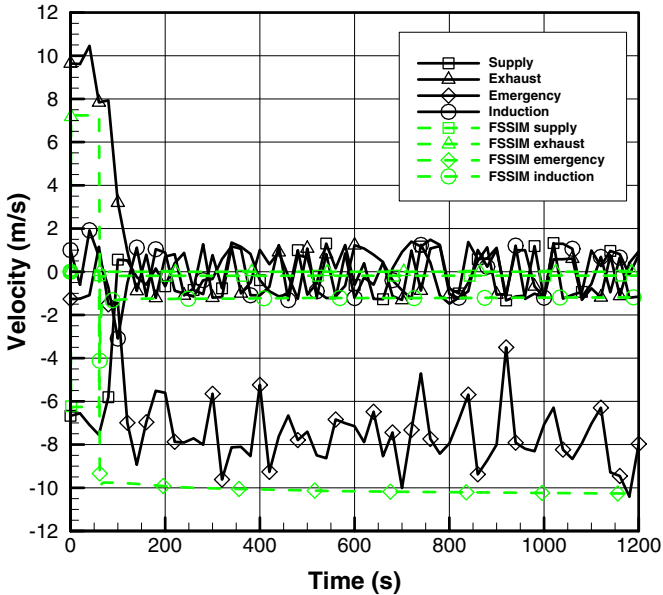


Figure 12. Predicted vs measured HVAC system velocities for Shadwell/688 test 5-14. (The color version of this figure is available on-line.)

CONCLUSIONS

A new software tool for modeling fire growth and smoke transport has been developed. The goal of the development was to create a stable program capable of modeling fires in complexly interconnected structures with multiple HVAC subsystems for the purpose of modeling shipboard fires. The limited validation shown in this paper demonstrates the accuracy and the capability of this new tool.

In a direct comparison with both CFAST and FDS, FSSIM performed well in predicting the averaged quantities for a single compartment with a fire and a vent opening. While, as expected, its predictions did not match the accuracy of FDS, FSSIM performed as well or better than CFAST in predicting compartment temperature change, vent mass flow, and neutral plane height.

A second validation was shown using the 688 submarine test area onboard the ex-*USS Shadwell*. The complexity of this test area would have been costly to model with FDS. The three separate ventilation systems and the complexity of their interactions exceeded the CFAST solver's ability to converge. FSSIM was capable of accurate, real-time computing of the spread of smoke and energy through the sub test area. Temperatures, gas concentrations, and mass flows were correctly predicted throughout the sub test area in both compartments and HVAC system components.

This first version of FSSIM is a success. It has met the goal of making accurate predictions of fire and smoke spread onboard a naval vessel. Further development of FSSIM, not covered in this paper, includes modeling detection and suppression systems, fire spread, progressive flooding, and runtime interaction with other software tools, including the automated extraction of geometric and systems information from digital design documents.

NOMENCLATURE

Roman

A = area (m^2)

c = specific heat ($J/(kg K)$)

c_p = constant pressure specific heat ($J/(kg K)$)

E = energy (J)

F = function or view factor

g = gravitational acceleration ($9.80665 m/s^2$)

h = enthalpy (J/kg) or heat transfer coefficient ($W/(m^2 K)$)

K = form loss factor
 k = thermal conductivity (W/(m K))
 L = length (m)
 M = mass (kg)
 mw = molecular weight (kg/mol)
 P = pressure (Pa)
 \dot{q} = heat transfer rate (W)
 R = real gas constant (8.314472 N m/(mol K))
 T = temperature (K)
 t = time (s)
 V = volume (m³)
 v = velocity (m/s)
 x = position (m)
 z = vertical position (m)

Greek

α = absorptivity (m⁻¹)
 β = miscellaneous multiplier (i.e., relaxation factor)
 Δ = change in
 ε = emissivity or wall roughness (m)
 ρ = density (kg/m³)
 σ = Stefan–Boltzman constant (5.6704 × 10⁻⁸ W/(m² K⁴)) or
 direction function (1 or -1)
 τ = transmission factor or time constant (s)

Superscripts

$''$ = per unit area (m⁻²)
 d = donor (upwind) quantity
 n = next time step
 $n+$ = next time step guess
 $n-$ = prior iteration
 $n-1$ = prior time step

Subscripts

air = air
 ex = exchange
 i = compartment
 j = junction
 k = compartment
 w = surface

Overscripts

$\dot{}$ = time derivative (s⁻¹)
 \sim = linearized value at next time step or modified net radiation
 term
 $\bar{}$ = averaged quantity

REFERENCES

1. Floyd, J.E., Hunt, S.P., Williams, F.W. and Tatem, P.A., Fire and Smoke Simulator (FSSIM) Version 1 – Theory Manual, NRL/MR/6180–04-8765, Naval Research Laboratory, Washington, DC, 2004.
2. Gaunt, R., Cole, R., Erickson, C., Gido R., Gasser, R., Rodriguez, S. and Young, M., MELCOR Computer Code Manuals: Reference Manuals Version 1.8.5, NUREG/CR-6119, US Nuclear Regulatory Commission, Vol. 2, Rev. 2, Washington, DC, 2000.
3. Williams, F., Nguyen, X., Buchanan, J., Farley, J., Scheffey, J., Wong, J., Pham, H. and Toomey, T., ex-USS Shadwell (LSD-15) – The Navy’s Full-Scale Damage Control and RDT&E Test Facility, NRL/MR/6180–01-8576, Naval Research Laboratory, Washington, DC, 2001.
4. Floyd, J., Scheffey, J., Haupt, T., Habbash, H., Hodge, B., Norton, O., Williams, F. and Tatem, P., Requirements and Development Plan for a Shipboard Network Fire Model, NRL Ltr. Rpt. Ser 6180/0469, Naval Research Laboratory, Washington, DC, 2003.
5. Dols, W., Walton, G. and Denton, K., CONTAMW 1.0 User Manual: Multizone Airflow and Contaminant Transport Analysis Software, NISTIR 6476, Building and Fire Research Laboratory, National Institute of Standards and Technology, Gaithersburg, MD, 2000.
6. Nichols, B.D. and Gregory, W.S., FIRAC User’s Manual: A Computer Code to Simulate Fire Accidents in Nuclear Facilities, NUREG/CR-4561 (LA-10678-M), Los Alamos National Laboratories for the Nuclear Regulatory Commission, 1986.
7. McGrattan, K., Forney, G., Floyd, J. and Hostikka, S., Fire Dynamics Simulator (Version 3) – User’s Guide, NISTIR-6784, 2002 ed., National Institute of Standards and Technology, Gaithersburg, MD, 2002.
8. Jones, W., Forney, G., Peacock, R. and Reneke, P., A Technical Reference for CFAST: An Engineering Tool for Estimating Fire Growth and Smoke Transport, NIST Technical Note 1431, National Institute of Standards and Technology, Gaithersburg, MD, 2000.
9. Childs, K.W., Heating 7.2 User’s Manual, ORNL/TM-12262, Oak Ridge National Laboratory, Oak Ridge, TN, 1993.
10. Cooper, L., Calculation of Flow Through a Horizontal Ceiling/Floor Vent, NISTIR 89-4052, National Institute of Standards and Technology, Gaithersburg, MD, 1989.
11. Holman, J., Heat Transfer, 7th ed., Mc-Graw Hill. New York, NY. 1990.
12. Strauss, W., Partial Differential Equations: An Introduction, John Wiley & Sons. New York, NY. 1992.
13. George, T., Wiles, L. Claybrook, S. Wheeler, C. McElroy, J. and Singh, A., GOTHIC Containment Analysis Package Technical Manual Version 7.0, EPRI RP4444-1, Electric Power Research Institute, Inc., Palo Alto, CA, 2000.
14. Forney, G., Computing Radiative Heat Transfer Occurring in a Zone Fire Model, NISTIR 4709, National Institute of Standards and Technology, Gaithersburg, MD, 1991.
15. Back, G., Mack, E., Peatross, M., Scheffey, J., White, D., Williams, F., Farley, J. and Satterfield, D., A Methodology for Predicting Fire and Smoke Spread Following a Weapon Hit, NRL/MR/6180–03-8708, Naval Research Laboratory, Washington, DC, 2003.
16. Wieczorek, C., Vandsburger, U. and Floyd J., “An Evaluation of the Global Equivalence Ratio Concept for Compartment Fires: Part I – Effect of Experimental Measurements,” Journal of Fire Protection Engineering, Vol. 14, No. 2, 2004, pp. 9–32.
17. Steckler, K., Quintiere, J. and Rinkinen, W., Flow Induced by Fire in a Compartment, NBSIR 82-2520, National Bureau of Standards (NIST), Gaithersburg, MD, 1982.
18. Steckler, K., Baum, H. and Quintiere, J., Flow Induced Flows Through Room Openings – Flow Coefficients, NBSIR 83-28010, National Bureau of Standards (NIST), Gaithersburg, MD, 1984.

19. Hoover, J., Tatem, P. and Williams, F., Meta-Analysis of Data from the Submarine Ventilation Doctrine Test Program, NRL/MR/6180—98-8168, Naval Research Laboratory, Washington, DC, 1998.
20. Parker, A., Scheffey, J., Hill, S., Farley, J., Tatem, P., Williams, F., Satterfield, D., Toomey, T. and Runnerstrom, E., Full-Scale Submarine Ventilation Doctrine and Tactics Tests, NRL/MR6810—98-8172, Naval Research Laboratory, Washington, DC, 1998.